

Initial stages of oxidation of Ge(111)- $c(2\times 8)$ studied by scanning tunneling microscopy

T. Klitsner

Sandia National Laboratories, Albuquerque, New Mexico 87185

R. S. Becker and J. S. Vickers*

AT&T Bell Laboratories, Murray Hill, New Jersey 07974

(Received 10 December 1990; revised manuscript received 19 February 1991)

The reaction of oxygen with the Ge(111)- $c(2\times 8)$ surface has been studied with use of a scanning tunneling microscope. Atomically resolved images of the same area before and after oxygen exposure reveal that, on a room-temperature surface, the primary nucleation sites are the boundaries between domains of different orientations of the $c(2\times 8)$ reconstruction. Point defects and disordered adatom regions can also act as nucleation sites. The $c(2\times 8)$ reconstructed terraces themselves and, unexpectedly, the step risers between terraces are found to be relatively unreactive. At elevated sample temperatures, the surface unreconstructs due to adatom mobility. At these elevated temperatures, the oxide nucleates homogeneously and pins the surface in a disordered adatom configuration. This suggests that facilitated oxidation at elevated sample temperatures is primarily due to degradation of the $c(2\times 8)$ reconstruction. Spectroscopic data from I - V curves are also presented and compared with known electronic spectra.

INTRODUCTION

While the intrinsic reconstructions of clean semiconductor surfaces have been studied for 30 years, no less interest has been displayed in the interaction of various atomic and molecular species with these surfaces. In particular, the interaction of molecular oxygen with Si (Refs. 1–8), and semiconductor surfaces in general is a subject of interest for both fundamental and technological reasons. Previous scanning tunneling microscopy (STM) studies include a study of the reaction of oxygen with GaAs(110) (Refs. 9 and 10) and, using a technique similar to the one used in the present work, several groups have studied the Si(111)- $(7\times 7)O_2$ system.^{5–8} Though there exists a small body of work on the reaction of germanium with oxygen,^{2,3,11–14} the amount of this work has been limited, presumably due to the fact that the oxide of germanium reacts with water rendering it technologically less useful. Nonetheless, understanding the surface properties of germanium is of fundamental interest, and in the case of the Ge(111)- $c(2\times 8)$ surface, we will argue that we have a model system for comparison to the more complicated Si(111) 7×7 surface. In addition technical interest in germanium has been increasing as heteroepitaxial growth techniques have improved,^{15–17} which have allowed unique electronic properties to be produced in Si/Ge alloys and superlattices.

While silicon and germanium have similar bulk structural and electronic properties, the behavior of their surfaces can be quite different. For instance, Si(111) forms the 7×7 reconstruction which is well described by the dimer–adatom–stacking-fault (DAS) model,¹⁸ while Ge(111) reconstructs in a $c(2\times 8)$ structure best described as adatoms arranged on the T_4 (closed) sites of a 1×1 surface.^{19–21} However, unlike Si(111), which forms

a stable oxide at room temperature, previous studies suggest that only a chemisorption oxygen state exists on the Ge(111) surface at room temperature, whereas the formation of a true oxide requires elevated temperatures.¹¹ In contrast to the DAS 7×7 reconstruction, which involves considerable subsurface rearrangement of atoms and bonds in the first double layer, the Ge(111) surface is a “softer,” purely adatom reconstruction with no subsurface rearrangement of atoms. In addition, the $c(2\times 8)$ does not have the threefold symmetry of the 7×7 . For these reasons Ge(111) tends to display a much greater amount of disordered domain boundaries between neighboring $c(2\times 8)$ regions than does the Si(111) 7×7 . Further, while the DAS structure naturally incorporates and reconstructs (112) steps into the surface structure, this is not so for the $c(2\times 8)$ structure. Rather, double-layer steps are ragged, with little tendency toward ordering along principle crystallographic directions and with no obvious reconstruction of the step riser. Despite these differences, these two reconstructions have certain geometric and electronic features in common; namely adatoms sitting on T_4 sites and nearly completely filled electronic bands associated with the rest-atom dangling bonds.^{22–24} By studying the initial stages of oxygen reaction on the simpler Ge(111)- $c(2\times 8)$ surface, we have a model system for studying the behavior of the *adatoms* on the 7×7 surface. It may then be possible to sort out the various aspects of this elementary reaction, determining which are due solely to the T_4 adatom structure and which are influenced by the subsurface stacking fault or dimer walls in the DAS structure.

In previous work on Ge(111), it was found that the sticking coefficient of oxygen dropped precipitously during the initial exposure.¹¹ Moderate increases in sample temperature (up to 250°C) were found to increase the

sticking coefficient somewhat. The sharp decrease in sticking coefficient with exposure was taken as evidence that the primary nucleation sites for oxygen reaction at room temperature were defect sites; the decrease in sticking coefficient being due to the saturation of these sites. Consistent with this supposition, high-flux electron bombardment, which is known to cause surface defects (albeit of unknown character), was found to increase the sticking coefficient. Furthermore, electron-energy-loss spectroscopy showed shifts in the Ge $3d$ core levels when the sample was exposed to oxygen at elevated temperatures, while at room temperature, no core-level shifts were observed though dangling-bond states were found to be saturated.^{2,11} Annealing a sample that was exposed to oxygen at room temperature was found to yield the same energy-loss spectrum and work functions that were obtained on samples exposed to oxygen at elevated temperatures. The core-level shifts were interpreted as charge transfer from Ge atoms to the more electronegative oxygen atoms, thus true oxidation appeared to occur only at elevated temperatures, while room-temperature exposure led only to chemisorption of oxygen with some saturation of the dangling bonds. Since elevated temperatures appear to be needed to produce an oxidized state and annealing can convert the chemisorbed surface to an oxidized one, it appears that some type of activation energy is needed for the oxidation process. Clearly, STM is a good tool for determining whether oxide nucleation does indeed occur at defect sites and, if so, what the nature of these defect sites might be. We will also show that STM can shed light on the nature of the activation energy for this reaction.

In this study we use a scanning tunneling microscope to image a particular area on a Ge(111)- $c(2\times 8)$ surface at atomic resolution both before and after dosing the surface with oxygen. Bias-dependent tunneling images give information on the spatial conformation of both filled and empty states on the surface, while we obtain spectroscopic information relating to the local density of states (LDOS) from tunnel junction I - V data. Initial STM work on the Si(111) 7×7 surface indicated that at room temperature, oxidation of Si(111) 7×7 could only be nucleated by missing adatom defects, while the reconstructed terraces and step risers were relatively insensitive to oxygen exposure.⁵ More recent work⁶⁻⁸ on Si(111) indicates that the oxidation occurs on apparently nondefect sites via at least a two-step process. In these studies it was found that the so-called "corner" and "center" adatoms had different reactivities, as did the faulted and unfaulted halves of the unit cell. On Ge(111) there are no stacking faults or dimer walls to introduce asymmetry between adatom sites. However, as we stated previously, there does exist a relatively large number of disordered domain boundaries between the different $c(2\times 8)$ orientations. We find, in the present study, that it is in fact these domain boundaries that act as the primary nucleation sites for oxygen reaction. As we noted before, such domain boundaries generally do not exist on the 7×7 surface due primarily to its threefold symmetry. We also find that adatom defects can nucleate oxidation on Ge(111). Reconstructed $c(2\times 8)$ terraces and step risers

on Ge(111) are found to be unreactive as seen on the Si(111) 7×7 , suggesting that these features are inherent to adatom surfaces in general and do not require the subsurface stacking fault or dimer walls of the DAS reconstruction. That the nucleation process occurs on terraces and not at double-layer steps on Ge(111) is quite surprising in view of the fact that Ge(111) steps are not strongly reconstructed in the fashion of Si(111) 7×7 steps. The implications of this observation will be addressed at greater length in the discussion of our results.

EXPERIMENT

The STM and vacuum system used has been described elsewhere.²⁵ Briefly, the STM is a four-quadrant tube design, mounted on a piezoelectric walker for coarse approach. The tunneling tip is polycrystalline tungsten, electrochemically etched and cleaned *in situ* by electron field emission. The ultrahigh-vacuum system has a base pressure of 5×10^{-11} Torr, and is equipped with a low-energy electron-diffraction (LEED) apparatus and an Auger electron spectrometer for measurement of average sample characteristics, as well as a residual gas analyzer (RGA), ion sputter gun for sample surface cleaning, and several controlled leak sources for gas dosing.

We prepared our initial surfaces by sputter cleaning the Ge(111) sample (Ne^+ , 1.0 keV) while direct current heating it to about 600°C, followed by 800°C 1-min anneals. This results in a sharp, low-background $c(2\times 8)$ LEED pattern, indicating a surface with generally large reconstructed domains. Tunneling images reveal large reconstructed terraces with occasional domain boundaries between $c(2\times 8)$ regions of different orientations.

Before the sample is exposed to O_2 , the tip is pulled back from the surface about 1.5 μm so that the tip, with a final radius of about 1000 Å, does not mask the sample surface. At this point, oxygen is admitted into the chamber through a leak valve while the ion pump is shut down. The ion gauge, which is in direct line of sight to the sample, is turned off in order to minimize effects due to the ionization of the molecular oxygen. The RGA, which is not in sample line of sight and has a much smaller filament, is used to monitor the oxygen partial pressure during dosing. A maximum partial pressure of 1×10^{-6} Torr O_2 is permitted. After the desired dose has been achieved, the oxygen is pumped from the chamber with the ion pump, and the tip is brought back into tunneling range. Typically, we find that the position of the tip is within 100 Å of its original location. Although we did not attempt to determine absolute dose levels, we point out that it is highly desirable to pull the tip back from the surface during the dosing to ensure that the tip does not occlude the area being studied or otherwise influence the adsorption process. For similar reasons, it may not be desirable to have the tip tunneling (or scanning) during the dosing, as was employed by certain other groups.

RESULTS

In Figure 1 we show the results of consecutive oxygen dosing on a 600×600 Å² area. The area contains several

terraces separated by single atomic steps and other surface features which simplify locating changes from dose to dose. The reaction process is clearly not homogeneous. As we go from 15 to 30 to 90 L (1 L = 10^{-6} Torr sec) we see that the $c(2\times 8)$ reconstructed areas and the step risers are relatively unaffected during the initial dosing; subsequently, the reaction spreads from nucleation sites associated with preexisting defects. Even at the highest exposures shown in this sequence (90 L), the $c(2\times 8)$ regions are largely unaffected. It should be emphasized that the information we obtain from the STM consists largely of changes we observe in the topography of the surface and changes in the contrast of the images

due to electronic effects. We have therefore primarily studied only the oxygen reactions that induce disorder on the surface. Our retarding-field Auger measurements of oxygen coverage correspond within a factor of 2 with coverages deduced from STM images. However, due to uncertainties in both our Auger measurements and in accounting for effects such as collateral disorder around reacted sites, we cannot rule out the possibility that oxygen chemisorption that does not produce disorder may be occurring over part of the surface. If this chemisorption produced electronic states out of the range of the bias voltages used in this study, these sites would not be apparent in our images. Therefore, when we refer to nu-

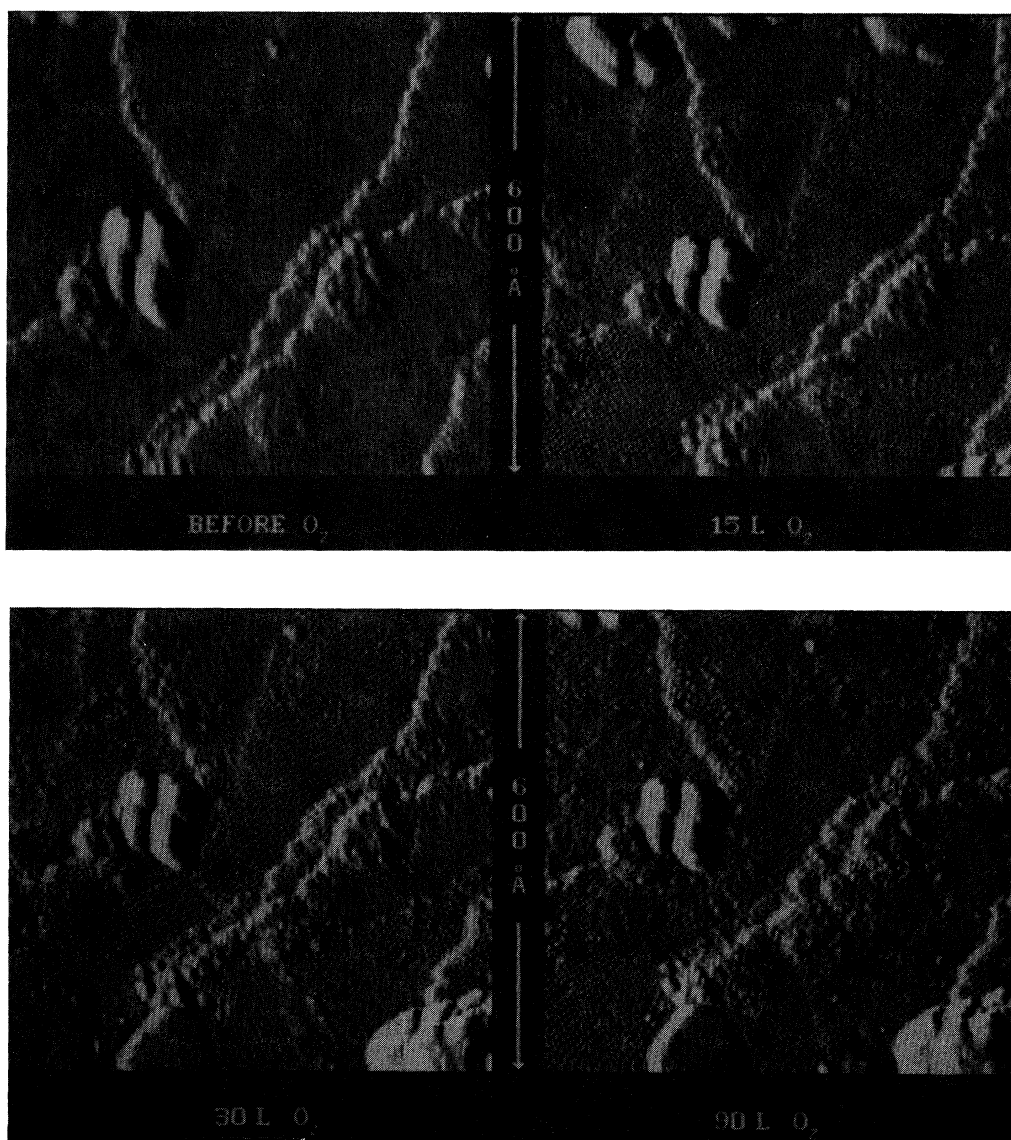


FIG. 1. Sequence of STM topographs on Ge(111) showing the progressive disordering effect of increasing oxygen exposure. The area imaged consists of a set of single atomic steps of $c(2\times 8)$ reconstruction descending from the bottom right to the top left of the image. This area was chosen because it has several features that can be used as a position reference from one topograph to the next. Note that even at the highest dose the step edges retain their shape.

cleation sites, we are referring to nucleation of the disorder-inducing reaction of oxygen with the surface. We will eventually associate this reaction with the initial stages of oxidation of the surface.

More information can be obtained by looking at higher-resolution tunneling images and by examining the

bias voltage dependence of these images. The various features of $c(2 \times 8)$ tunneling images are described in detail in Becker *et al.*¹⁹ Briefly, the electronic features on the $c(2 \times 8)$ are dominated by dangling-bond states. Because the rest-atom dangling-bond state is lower in energy than the adatom dangling-bond state, there is charge

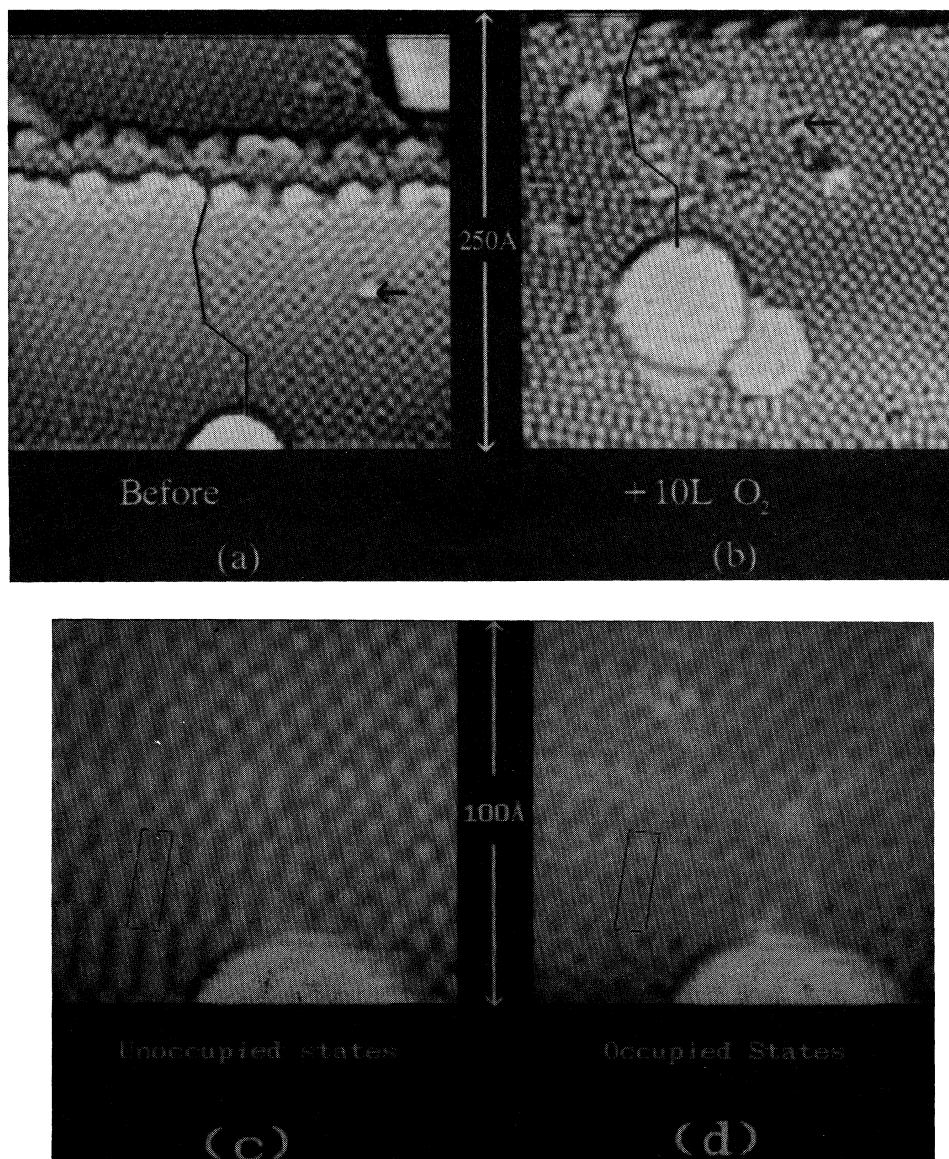


FIG. 2. (a) Disordered boundary (denoted by the jagged line) between two $c(2 \times 8)$ domains of different orientations before oxygen dosing. The bright mound in the lower part of the topograph can be used as a position reference in subsequent images. (b) Same region as (a) after 10 L O_2 dosing. Note that while the region around the domain boundary has become quite disordered, the $c(2 \times 8)$ regions seem relatively inert. (c) Higher-resolution image of the domain boundary before oxygen dosing. Image taken at +1.8 V tunneling into unoccupied surface states, which have previously been identified with the position of the adatoms on Ge(111)- $c(2 \times 8)$. (d) Image taken simultaneously with (c) at -1.8 V tunneling out of occupied surface states. For Ge(111)- $c(2 \times 8)$, both rest-atom and adatom sites are imaged at this polarity. (e) Domain boundary after 10 L O_2 dosing. Unoccupied-state image taken at +1.8 V. The edge of the circular mound can be seen at the very bottom of the topograph for position reference. Besides disordering occurring, there are several features that appear as dark depressions in this unoccupied-state image. (f) Occupied-state image taken simultaneously with (e) at -1.8 V. Note that many of the features which appeared as depressions in (e) appear as bright protrusions in the occupied-state image.

transfer from the adatom to the rest-atom sites on the equilibrium surface.^{22–24} This is also true on a 7×7 reconstructed surface. On the 7×7 surface, however, there are more adatoms than rest atoms due to the dimer walls incorporated into the reconstruction. Therefore only partial charge transfer is possible. The adatoms then have partially filled dangling-bond states and are imaged at both positive and negative polarity. For the $c(2\times 8)$ [or the related 2×2 and $c(4\times 2)$] structure, there is a one-to-one correspondence between the number of adatom and rest-atom dangling bonds. There is then more complete charge transfer leading to a nearly empty band associated with the adatom dangling bonds and a nearly full one associated with the rest-atom dangling bonds. Unoccupied-state images therefore correspond to adatom positions, while rest atoms show up more prominently in the occupied-state images. Surface structures which break the (2×2) -like symmetry of the surface (such as $\sqrt{3}$ adatom spacing) can lead to a local excess of adatoms. This in turn again leads to partially filled adatom dangling bonds, which will then show up prominently at both tunneling polarities, much like what is observed for the 7×7 structure.

Figure 2(a) is a 250-Å tunneling image showing a domain boundary (delineated by the jagged line) between two $c(2\times 8)$ domains prior to exposure to molecular oxygen. The bright moundlike feature can be used as a position reference in this and subsequent images. Figures 2(c) and 2(d) show simultaneously obtained dual polarity, high-resolution images of the same region. After dosing with 10 L of O_2 we recorded the tunneling image shown in Fig. 2(b). Higher-resolution, dual-polarity images of the domain boundary region after oxygen exposure are shown in Figs. 2(e) and 2(f). Figure 2(b) clearly shows that the $c(2\times 8)$ regions are relatively unaffected by the dosing, while the area in and adjacent to the domain boundary has reacted. This is in accordance with previous studies¹² of this system using LEED as well as our

own LEED observations which show that the $c(2\times 8)$ diffraction pattern is unaffected during the initial stages of oxygen dosing.

Figures 2(e) and 2(f) [as well as 2(c) and 2(d)] were acquired at ± 1.8 V bias while tunneling, respectively, into unoccupied sample states and out of occupied sample states. The reacted area appears predominantly as depressions when tunneling into unoccupied states and as protrusions when tunneling out of occupied sample states. This is in qualitative agreement with previous work^{9,10,26} which indicated that the more electronegative oxygen atom should cause a reduction of state density above the Fermi level and a corresponding increase in state density below the Fermi level. The feedback loop of the STM then responds to these changes in LDOS by moving the tip in or out, producing depressions or protrusions in the image. Other images, however, can show reacted regions as either protrusions or depressions at both tunneling polarities. While it is possible, in these cases, that an etching process has occurred, resulting in the evolution of GeO_x , the fact that STM images are dominated by spatial variations in the density of states suggests that the electronic structure is simply more complicated than this qualitative picture of simple charge transfer to an electronegative adsorbate.

Figures 2(e) and 2(f) also show that even the apparently unreacted areas around this region are becoming more disordered, with previously $c(2\times 8)$ ordered adatoms arrayed in 2×2 and $c(4\times 2)$ local symmetry. This tendency towards disorder adjacent to oxygen-reacted areas appears to play an important role in the adsorption process. Domain boundaries and defects nucleate the reaction, inducing a disordering of the neighboring $c(2\times 8)$ reconstructed regions. We find that these newly disordered regions can then serve as nucleation sites for further reaction.

This tendency for collateral disorder to occur around reacted regions raises an interesting point. Previous

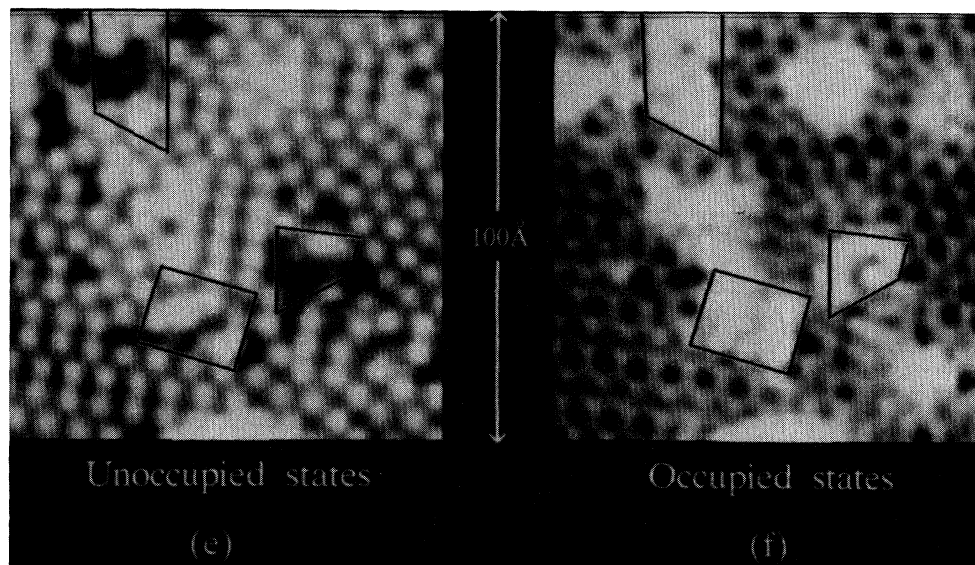


FIG. 2. (Continued).

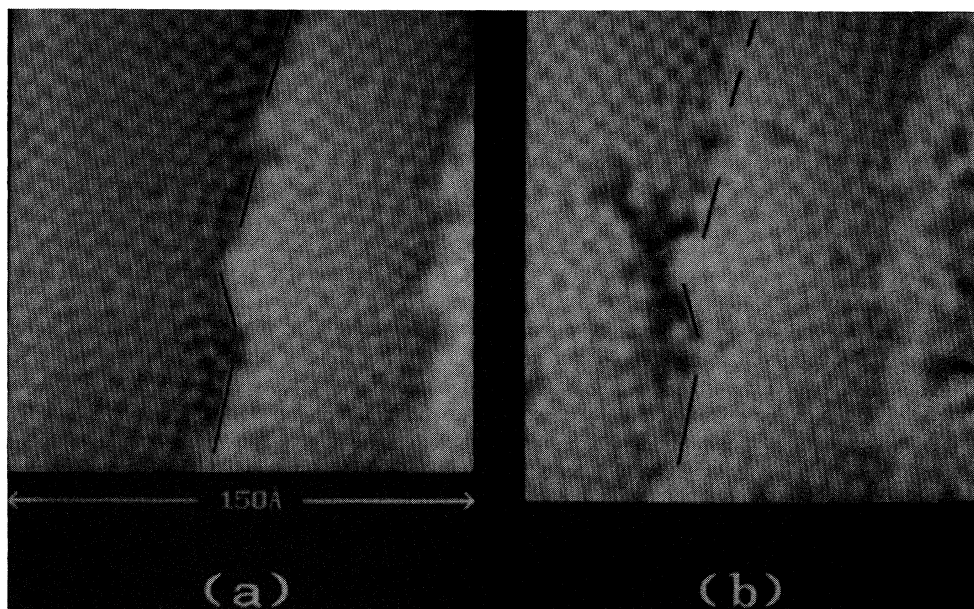


FIG. 3. (a) Topograph taken before dosing with O_2 , showing a set of single atomic steps descending from the right to the left of the image. (b) Steps after 10 L O_2 dose. Note that, while the disordered regions adjacent to the step edges have reacted, the step edge itself has retained its shape and atomic positions.

work¹¹ has shown that at room temperature the sticking coefficient drops sharply during the initial oxygen exposure. Our own Auger work also confirms that the oxygen coverage is saturating at about 0.2 monolayer with continued dosing. This is consistent with reaction at defect sites as we observe in our STM images. However, if more disordered sites are created during the reaction, as we observe, one might expect that the number of nucleation sites could be increasing instead of saturating. To resolve this issue, it is necessary to take STM images after very high doses of oxygen. Because, in addition to the surface, the STM tip can also react, we found we had an effective dosing limit of about 100 L. In addition, we have made no attempt to calibrate the actual dose reaching the part of the sample under study. For these reasons, we cannot with confidence determine a sticking coefficient or discern whether or not the reaction rate, as determined from STM observations, is in fact saturating.

In Fig. 3(a) we show a set of single atomic steps descending from right to left with disordered regions and phase boundaries on the step terraces adjacent to the step edges. Figure 3(b) shows the region after 10 L oxygen exposure. These images show the relative insensitivity of the step risers to oxygen exposure. That is, while the domain boundaries and disordered regions adjacent to the step edges have reacted as before, the step edges themselves have retained their shape. In fact, one can follow the step edges atom by atom and see that, surprisingly, almost none of the atoms has changed positions during the oxygen exposure. As stated previously, steps on Ge(111)- $c(2 \times 8)$ tend to be quite ragged and need not strictly follow principle crystallographic directions, which suggests that there is little if any reconstruction of the step edge. However, the insensitivity of these step

risers to oxygen exposure seems to indicate that, contrary to previous evidence, there is indeed at least some local reconstruction of the step riser. That is, if we assume that the more disordered regions on the sample are more reactive due to energetically less favorable distributions of charge transfer between dangling bonds, then the relative inertness of the step risers indicates that some reconstruction at the step edge is occurring to reduce the number of unsatisfied dangling bonds.

We have also obtained data on surfaces that are held at elevated temperatures during oxygen exposure. Here we raise the temperature of the sample until the fractional order spots in the $c(2 \times 8)$ LEED pattern vanish. This occurs at about 300 °C.^{12,27} At this point 1 L of oxygen is admitted into the chamber. After the oxygen is pumped out, the sample is allowed to return to room temperature, and STM images can be obtained. Our LEED measurements for samples exposed in this way reveal a somewhat diffuse 1×1 pattern. Our STM results are shown in Fig. 4 and explain this LEED observation. At this temperature, the Ge(111) surface apparently does not revert to a true 1×1 bulk terminated structure, but rather converts to a disordered adatom configuration. Under these conditions, the Ge(111) surface reacts homogeneously with oxygen and is pinned in this disordered adatom configuration upon cooling. It is, perhaps, not surprising that the surface would react homogeneously at this temperature. Since the $c(2 \times 8)$ order is destroyed as the adatoms become more mobile, there are no longer any domain boundaries to act as preferential nucleation sites. The entire Ge(111) surface is now similar in structure to one large domain boundary, presenting a homogeneous target for incoming oxygen molecules rather than the inhomogeneous target the room-temperature surface

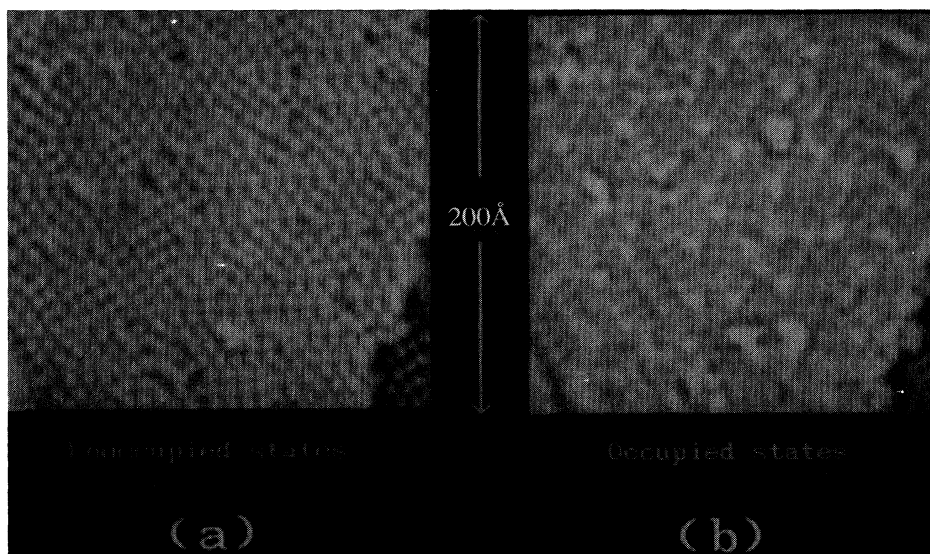


FIG. 4. Topograph taken after 1 L dose of O_2 on a surface that was held at $300^\circ C$ during the dosing. At this temperature, the $c(2\times 8)$ reconstruction becomes disordered due to adatom mobility. The surface then reacts homogeneously and is pinned in a random adatom configuration.

presents. In addition, our data on surfaces exposed to oxygen at room temperature show that the disordered adatom regions are the most reactive. The degradation of the $c(2\times 8)$ order that occurs at elevated temperatures would then be expected to increase the reactivity of the surface. As we stated in the Introduction, previous work has suggested that true oxidation of germanium, involving charge transfer, occurs only at elevated temperatures. We suggest that this is not strictly true. It appears that the primary factor governing surface reactivity is the $c(2\times 8)$ ordering of the adatoms. True oxidation may occur on room-temperature surfaces, but only over those relatively small areas that are somewhat disordered, such as the domain boundaries. The rest of the ordered room-temperature-exposed surface may have areas with chemisorbed oxygen, but not be truly oxidized. This would account for the measured electronic spectra, which naturally represent the global, coherent properties of the surface rather than the properties of the small disordered regions. It appears, then, that rather than oxidation itself being an activated process, it is the reconstruction change that is "activated" with the subsequent degradation of the $c(2\times 8)$ order leading to the increased reactivity of the surface.

Spectroscopic data obtained from STM current-voltage (I - V) characteristics are shown in Fig. 5. We show data obtained over a nonreacted $c(2\times 8)$ domain along with data over a reacted region. The I - V data taken on reacted regions can vary somewhat depending on the specific site being sampled and the state of the tunneling tip,^{28,29} but the data presented here represent some common features. The first thing to note is that the spectrum taken over the unreacted region is distinctly semiconducting, while the spectrum taken over the reacted region has more of the metallic character that is seen for the 7×7 reconstruction. The semiconducting character of the unreacted $c(2\times 8)$ is due to the strong spatial separation of

the occupied and unoccupied states on this surface. As we described earlier, this leads to a nearly filled band associated with the rest-atom dangling bond, and a nearly empty band associated with the adatom dangling bond. When the (2×2) -like symmetry of the surface is broken, the dangling bonds become partially filled, just as in the case of adatoms in the 7×7 reconstruction, and the surface takes on the observed metallic aspect. The most pronounced feature in the spectrum taken over the nonreacted region are the peaks at $\sim \pm 0.5$ eV, which previously

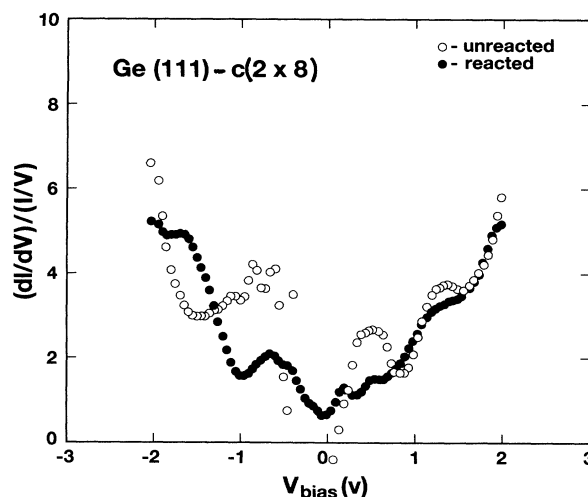


FIG. 5. Spectroscopic I - V data taken over reacted and unreacted areas. While the unreacted region is distinctly semiconducting, the reacted region is more metallic. The diminishing of the peaks at $\sim \pm 0.5$ V over the reacted region may be related to saturation of the dangling bond. The presence of the peak at ~ -1.5 V over the reacted region may be associated with previously observed shifts in the backbond state.

have been associated with the dangling-bond states.¹⁹ These peaks are attenuated in the data taken over the reacted region. This is consistent with previous spectroscopic results on this system showing saturation of the dangling-bond states upon initial exposure to oxygen.¹¹ The peak at ~ -1.5 eV may be associated with a shift in energy of the state associated with the Ge backbond, which has also been reported to occur upon oxidation.

In summary, we have shown that the boundaries between $c(2\times 8)$ domains are the primary nucleation sites for oxygen reaction on the room-temperature Ge(111) surface. Defects and other disordered regions can also nucleate the reaction, but step edges are surprisingly inert. The lack of reactivity at the step edges suggests that they are, at least locally, reconstructed. The reaction process increases the mobility of adatoms around the nucleation sites, creating disordered regions that can act, at least to some extent, as subsequent nucleation centers. The enhanced reactivity of defects and disordered regions

and the relative lack of reactivity at step edges are features also seen in the oxidation of Si (7×7). This suggests that these common features are a property of adatoms on a 1×1 lattice, rather than features associated with the subsurface stacking fault or dimer walls that exist on the 7×7 surface. Rather than being an activated process itself, it appears that oxidation is facilitated at elevated temperatures primarily due to the degradation of the $c(2\times 8)$ order. Spectroscopic data are in general agreement with previous electronic spectra and support our suggestion that oxidation can occur on the disordered adatom regions at room temperature as well as at elevated temperatures.

ACKNOWLEDGMENTS

This work was performed while one of us (T.K.) was at AT&T Bell Laboratories and was partly supported by DOE Contract No. DE-AC04-76DP00789.

*Present address: Department of Physics, University of California at Berkeley, Berkeley, CA.

¹P. Morgen, V. Hofer, W. Wurth, and E. Umbach, *Phys. Rev. B* **39**, 3720 (1989).

²R. Ludeke and A. Koma, *Phys. Rev. Lett.* **18**, 1170 (1975).

³C. M. Garner, I. Lindau, J. N. Miller, P. Pianetta, and W. E. Spicer, *J. Vac. Sci. Technol.* **14**, 372 (1977).

⁴J. E. Rowe, G. Margaritondo, H. Ibach, and H. Froitzheim, *Solid State Commun.* **20**, 277 (1976).

⁵F. M. Leibsle, A. Samsavar, and T.-C. Chiang, *Phys. Rev. B* **3**, 5780 (1988).

⁶J. P. Pelz and R. H. Koch, *Phys. Rev. B* **42**, 3761 (1990).

⁷In-Whan Lyo, Ph. Avouris, B. Schubert, and R. Hoffmann, *J. Phys. Chem.* **94**, 4400 (1990).

⁸H. Tokumoto, K. Miki, H. Murakami, H. Bando, M. Ono, and K. Kajimura, *J. Vac. Sci. Technol. A* **8**, 255 (1990).

⁹J. A. Strosio, R. M. Feenstra, and A. P. Fein, *Phys. Rev. Lett.* **58**, 1668 (1987).

¹⁰J. A. Strosio, R. M. Feenstra, D. M. Newns, and A. P. Fein, *J. Vac. Sci. Technol. A* **6**, 499 (1988).

¹¹L. Surnev, *Surf. Sci.* **110**, 439 (1981).

¹²B. Z. Ol'shanetskii, N. I. Makrushin, and A. I. Volokitin, *Fiz. Tverd. Tela (Leningrad)* **14**, 3175 (1972) [*Sov. Phys.—Solid State* **14**, 2713 (1973)].

¹³G. B. Demidovich and A. A. Skylankin, *Vestn. Mosk. Univ. Fiz. Astronomiya* **35**, 96 (1980).

¹⁴G. V. Gadiyak, Yu. N. Morokov, and S. M. Repinskii, *Fiz. Tekh. Poluprovodn.* **12**, 1228 (1978). [*Sov. Phys.—Semicond.* **12**, 731 (1978)].

¹⁵J. C. Bean, *Science* **230**, 127 (1985).

¹⁶*Silicon-Molecular Beam Epitaxy*, edited by E. Kaspar and J. C. Bean (CRC, Boca Raton, FL, 1988), Vols. I and II.

¹⁷S. S. Iyer and F. K. Legoues, *J. Appl. Phys.* **65**, 4693 (1989).

¹⁸K. Takayanagi, Y. Tanishiro, S. Takahashi, and M. Takahashi, *Surf. Sci.* **164**, 367 (1985).

¹⁹R. S. Becker, B. S. Swartzentruber, J. S. Vickers, and T. Klitsner, *Phys. Rev. B* **39**, 1633 (1989).

²⁰R. Feidenhansl, J. S. Pedersen, J. Bohr, M. Nielsen, F. Grey, and R. L. Johnson, *Phys. Rev. B* **38**, 9715 (1988).

²¹P. M. J. Maree, K. Nakagawa, J. F. van der Veen, and R. M. Tromp, *Phys. Rev. B* **38**, 1585 (1988).

²²J. E. Northrup, *Phys. Rev. Lett.* **57**, 154 (1986).

²³R. D. Meade and D. Vanderbilt, *Phys. Rev. B* **40**, 3905 (1989).

²⁴T. Klitsner and J. S. Nelson (unpublished).

²⁵R. S. Becker, J. A. Golovchenko, and B. S. Swartzentruber, *Phys. Rev. Lett.* **54**, 2678 (1985).

²⁶N. D. Lang, *Phys. Rev.* **58**, 45 (1987).

²⁷R. J. Phaneuf and M. B. Webb, *Surf. Sci.* **164**, 167 (1985).

²⁸T. Klitsner, R. S. Becker, and J. S. Vickers, *Phys. Rev. B* **41**, 3837 (1990).

²⁹R. M. Tromp, E. J. Van Loenen, J. E. Demuth, and N. D. Lang, *Phys. Rev. B* **37**, 9042 (1988).

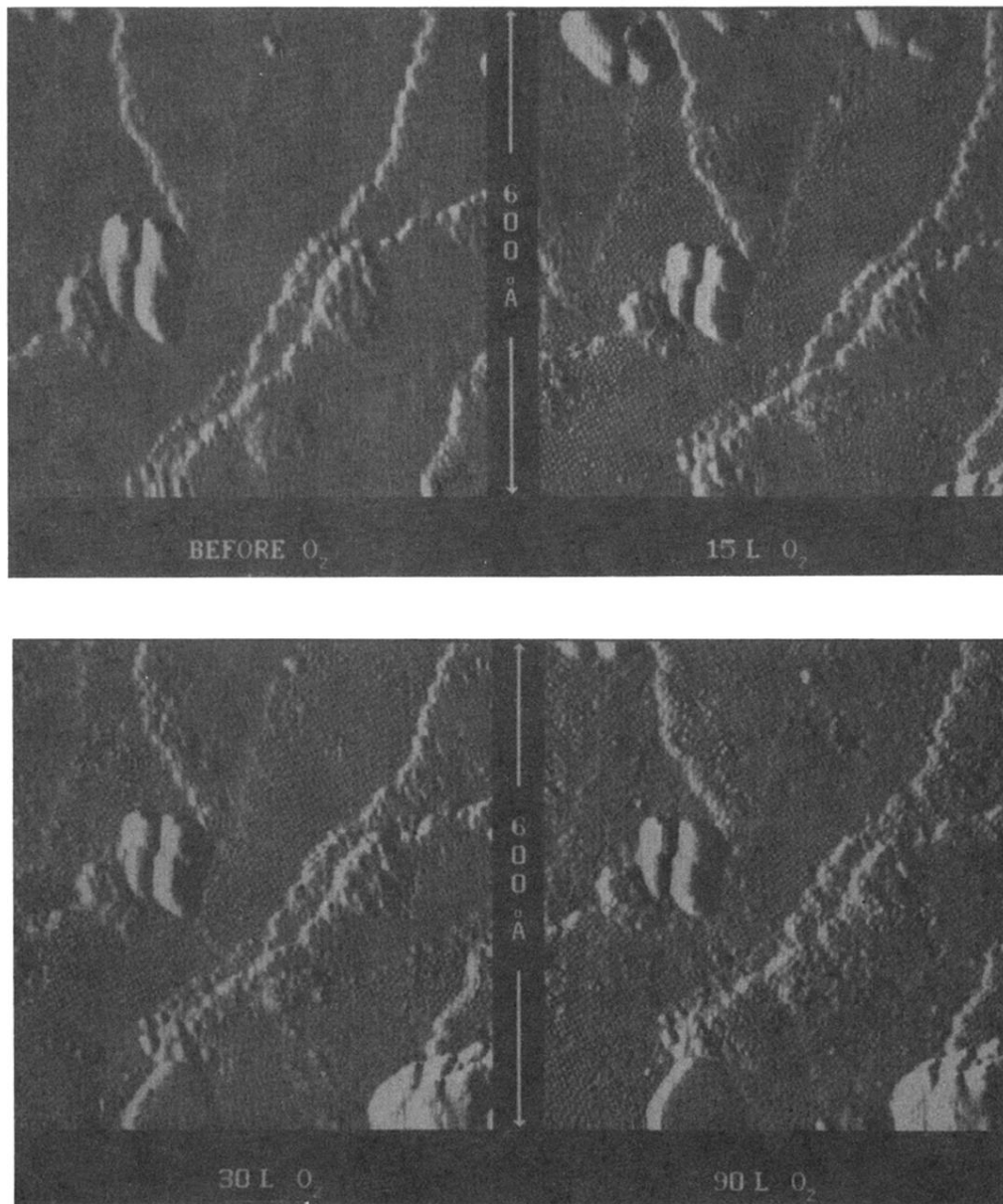


FIG. 1. Sequence of STM topographs on Ge(111) showing the progressive disordering effect of increasing oxygen exposure. The area imaged consists of a set of single atomic steps of $c(2 \times 8)$ reconstruction descending from the bottom right to the top left of the image. This area was chosen because it has several features that can be used as a position reference from one topograph to the next. Note that even at the highest dose the step edges retain their shape.

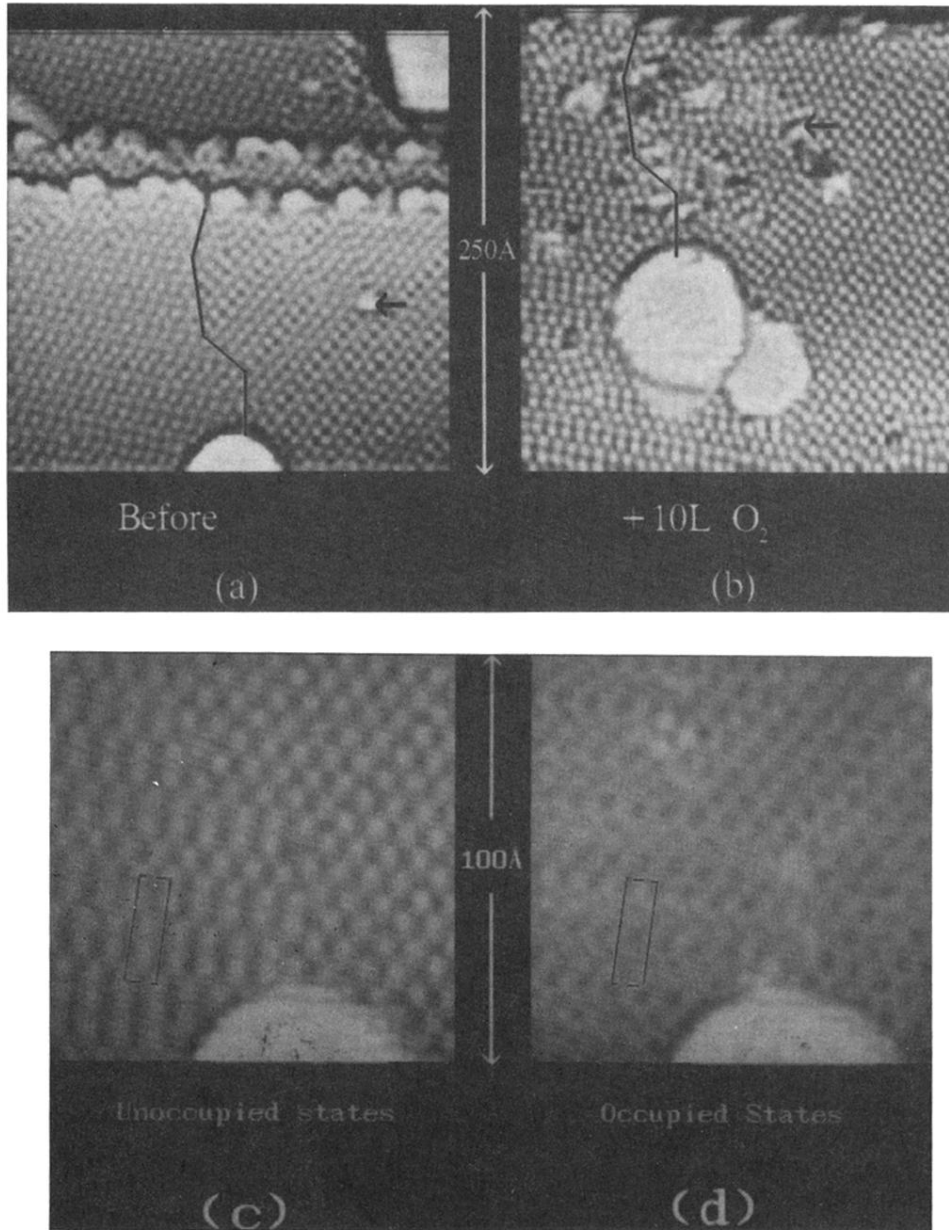


FIG. 2. (a) Disordered boundary (denoted by the jagged line) between two $c(2 \times 8)$ domains of different orientations before oxygen dosing. The bright mound in the lower part of the topograph can be used as a position reference in subsequent images. (b) Same region as (a) after 10 L O_2 dosing. Note that while the region around the domain boundary has become quite disordered, the $c(2 \times 8)$ regions seem relatively inert. (c) Higher-resolution image of the domain boundary before oxygen dosing. Image taken at +1.8 V tunneling into unoccupied surface states, which have previously been identified with the position of the adatoms on Ge(111)- $c(2 \times 8)$. (d) Image taken simultaneously with (c) at -1.8 V tunneling out of occupied surface states. For Ge(111)- $c(2 \times 8)$, both rest-atom and adatom sites are imaged at this polarity. (e) Domain boundary after 10 L O_2 dosing. Unoccupied-state image taken at +1.8 V. The edge of the circular mound can be seen at the very bottom of the topograph for position reference. Besides disordering occurring, there are several features that appear as dark depressions in this unoccupied-state image. (f) Occupied-state image taken simultaneously with (e) at -1.8 V. Note that many of the features which appeared as depressions in (e) appear as bright protrusions in the occupied-state image.

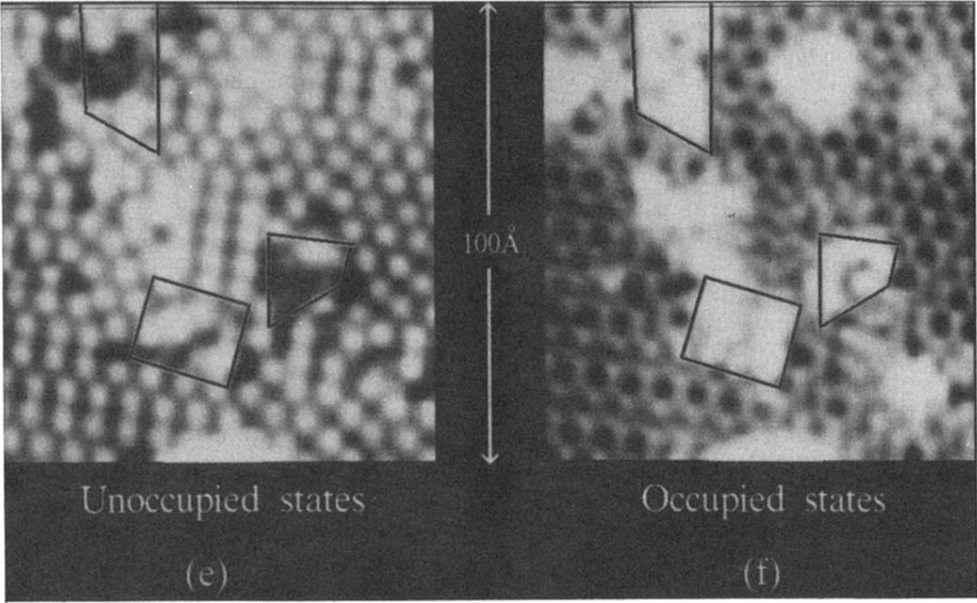


FIG. 2. (Continued).

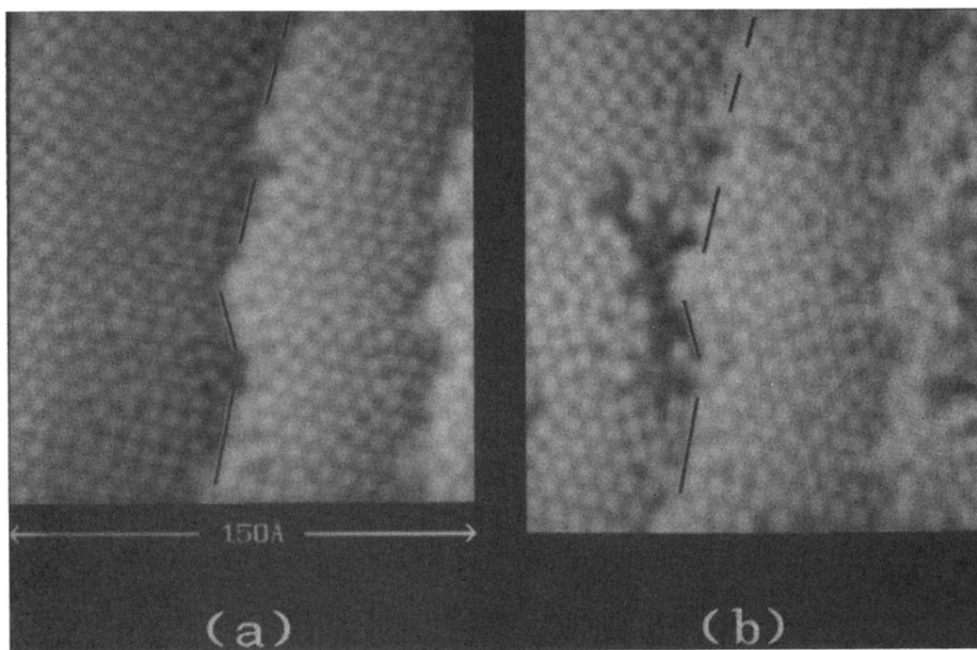


FIG. 3. (a) Topograph taken before dosing with O₂, showing a set of single atomic steps descending from the right to the left of the image. (b) Steps after 10 L O₂ dose. Note that, while the disordered regions adjacent to the step edges have reacted, the step edge itself has retained its shape and atomic positions.

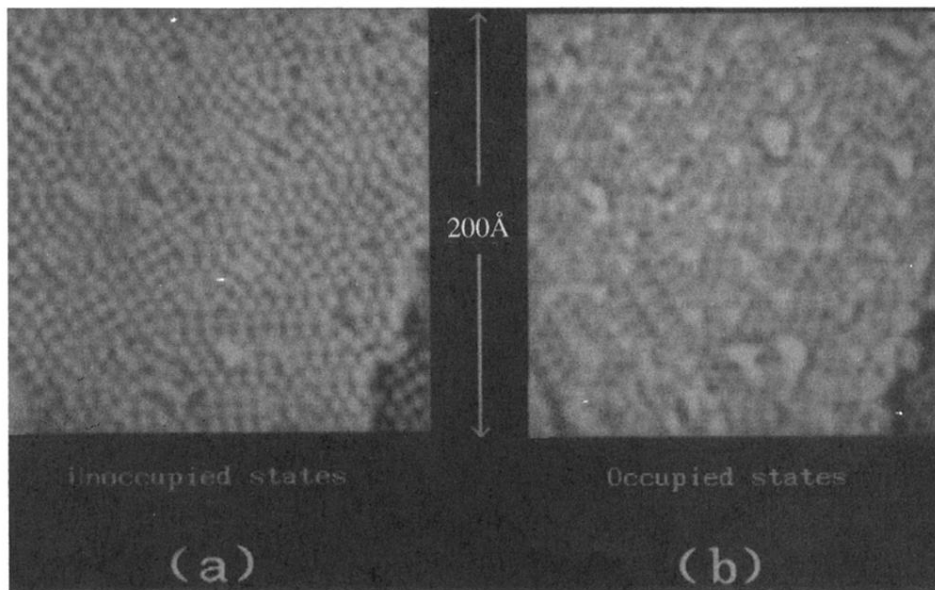


FIG. 4. Topograph taken after 1 L dose of O_2 on a surface that was held at 300°C during the dosing. At this temperature, the $c(2\times 8)$ reconstruction becomes disordered due to adatom mobility. The surface then reacts homogeneously and is pinned in a random adatom configuration.